Extreme springs in Switzerland since 1763 in climate and phenological indices

Noemi Imfeld[1,2], Koen Hufkens[1,2], and Stefan Brönnimann[1,2]

[1]Oeschger Center for Climate Change Research, University of Bern, Switzerland
[2]Institute of Geography, University of Bern, Switzerland

Correspondence: Noemi Imfeld (noemi.imfeld@unibe.ch)

Abstract. Historical sources report manifold on hazardous past climate and weather events that had considerable impacts on society. Studying changes in the occurrence or mechanisms behind such events is, however, hampered by a lack of spatially and temporally complete weather data. Especially, the spring season has received less attention in comparison to summer and winter, but is nevertheless relevant since weather conditions in spring can delay vegetation and create substantial damage due to
5 for example late frost events. For Switzerland, we created a daily high-resolution (1x1 km^2) reconstruction of temperature and precipitation fields from 1763 to 1960, that forms together with present-day meteorological fields a 258-year-long gridded data set. With this data set, we study changes in longer-term climate and historical weather events based on climate and phenological indices focusing on the spring season.

Climate and phenological indices show few changes in the mean during the first 200 years, but climate change signals clearly
10 emerge in all indices in the most recent period. We evaluate the climate and phenological indices for three cases of extreme spring weather conditions, an unusually warm spring, two late frost events, and three cold springs. Warm springs are much more frequent in the 21st century, but also in 1862 a very warm and early spring occurred. Spring temperatures, however, do not agree on how anomalously warm the spring was when comparing the Swiss reconstruction with reanalyses that extend back to 1868. The three springs of 1785, 1837, and 1853, were particularly cold with historical sources reporting for example
15 prolonged lake freezing and abundant snowfall. Whereas the springs of 1837 and 1853 were characterized by cold and wet conditions, in the spring of 1785 wet-days were below average and, in particular, in the Swiss Plateau, frost days reached an all-time maximum. Such inversion conditions are confirmed by mostly north-easterly and high pressure weather types and historical sources describing prolonged Bise conditions. Studying such historical events is valuable since similar atmospheric conditions can also nowadays lead to cold springs affecting vegetation growth and agricultural production.

20 ## 1 Introduction

Studies of long-term climate variability often focus on the summer or winter season. However, climate in spring is equally important, for example, for plant growth, and may have far reaching impacts. Cold spells in spring can delay crop growth considerably, late frost events can destroy harvests, and spring snowfall may put trees at risk. Moreover, late beech leaf unfolding may prolong the spring wildfire season as sunlight penetrates to the ground and dries the litter layer. Studying such

25 adverse weather conditions in spring requires daily data, from which targeted climate indices can be calculated. Studies have evaluated changes in climate indices over the last few decades (e.g. Brown et al., 2010; Domínguez-Castro et al., 2020; Zhang et al., 2011), also focusing specifically on spring conditions, such as changes in late frost occurrence and safety margins of plants (e.g. Wypych et al., 2017; Vitasse et al., 2018). Only very few studies, however, extended analyses of daily-based climate indices across several centuries because the temporally complete daily data that is needed is scarcely available (Brugnara

30 et al., 2022; Parker et al., 1992; Diodato et al., 2020). In particular from a historical perspective evaluating daily-based indices, such as the occurrence of frost days or the occurrence of the last frost day in spring can be relevant as they are often reported in historical documents (Zhang et al., 2011; Pfister et al., 2017). Studying historical weather conditions in spring may also contribute to our understanding of adverse spring weather since it extends the sample of extreme events.

For Switzerland, we created a daily high-resolution (1x1 km^2) reconstruction of temperature and precipitation fields from

35 1763 to 1960 (Imfeld et al., 2023b), that forms together with present-day meteorological fields a 258-year-long gridded data (MeteoSwiss, 2021a, b). This data set allows us to calculate impact-relevant climate and phenological indices for the 258-year-long period and to study longer-term climate and past extreme springs since 1763. A dense network of phenological observations exists in Switzerland starting in 1951 (Auchmann et al., 2018; Brugnara et al., 2020a), but for earlier periods, historical phenological observations are sparse. Thus, we used numerical approaches to model phenology from the gridded

40 daily meteorological data.

This article is organized as follows. In Sect. 2, we describe the meteorological data used to calculate climate and phenological indices. In Sect. 3, we describe the calculation of the climate indices and the phenological application. In Sect. 4, we describe the long-term changes in the climate and phenological indices, and analyze these indices for three different extreme spring cases, a warm spring, two frost events, and three cold springs. These results are discussed in Sect. 5. In Sect. 6, we conclude

45 our article.

2 Data

2.1 Meteorological data

For the calculation of climate and phenological indices, we used a reconstruction of 258 years of daily mean temperature and daily precipitation sums for Switzerland covering a period from 2 January 1763 to 31 December 2020 with a resolution of 1

50 km (Imfeld et al., 2023b). For precipitation, the gridded dataset also covers catchment areas outside Switzerland. These meteorological fields were reconstructed with the analog resampling method, quantile mapping, and data assimilation. The analog resampling and data assimilation are performed using a large number of instrumental measurement series from Switzerland and neighbouring regions. The data sets consist of two main sub-periods with different reconstruction skills due to the availability and quality of the input data. From 1763 to 1864, the reconstruction shows good skills for daily temperature with correlations

55 on average between 0.80 and 0.96 (calculated from the anomalies of a climatological annual cycle) and root mean squared errors on average between 1 and 2.6 °C depending on the input station network and season. For precipitation, the reconstruction skill for the period from 1763 to 1864 is considerably lower with correlations on average between 0.6 and 0.8 and root mean

squared errors between 6 and 10 mm depending on station network and season. However, the number of monthly wet days compares well to independent observations. After 1864, reconstruction skills are much improved across Switzerland for both

60   temperature and precipitation data. Despite the drawbacks in the early period, we used this novel data set, since it is the first one offering daily data at a high spatial resolution. A detailed description of the reconstruction is found in Imfeld et al. (2023b).

2.2   Reanalyses and weather types

In addition, we used the station-based daily temperature time series for the Swiss plateau derived from the series of Bern and Zurich (Brugnara et al., 2022), further denoted as the "Swiss series", the reanalysis 20CRv3 starting in 1807 (Slivinski

65   et al., 2019), and the Modern Era Reanalysis ModE-RA (Valler et al., in review) to calculate the same indices. Note that these data sets are not fully independent of the Swiss reconstruction since they all rely partly on the same input data. From the reanalysis 20CRv3, we selected out of the four closest grid cells, the cell that correlates well and had a low bias compare to the Swiss Plateau area mean value. For ModE-RA, we used the grid cell in the northwest of Switzerland because it had a low biases in comparison to the Swiss Plateau area mean. 20CRv3 assimilates pressure observations from Hohenpeissenberg,

70   Torino, and Geneva, which are also used in the Swiss reconstruction (Imfeld et al., 2023b), whereas ModE-RA assimilates pressure, temperature, and wet-days, but on a monthly resolution. 20CRv3 and ModE-RA were further used to analyze similar atmospheric conditions during the extreme spring examples. To evaluate the occurrence of weather types, we considered the reconstruction of Schwander et al. (2017) starting in 1763.

3   Methods

75   ## 3.1   Climate indices

We selected eight different climate indices for daily mean temperature and precipitation (Tab. 1, upper row) which have been suggested by the Expert Team on Climate Change Detection and Indices (ETCCDI) (e.g. Zhang et al., 2011). They are not exclusively based on spring weather, i.e. some are influenced already by winter temperatures, but they generally relate to conditions in spring. Because only daily mean temperature is available for the period since 1763, we adjusted the indices to

80   daily mean temperature. A frost day was defined as a day with a daily mean temperature below 0 °C. Such a day is thus colder than what is normally considered a frost day. The warm and cold spell indices were calculated for the 10th and 90th percentile thresholds in the reference period of 1871 to 1900 for daily mean temperature and not minimum and maximum temperature. Snowfall days were calculated according to Zubler et al. (2014) using a threshold of at least 1 mm for precipitation and less than 2 °C for daily mean temperature. Further, we calculated the growing season start based on the first six days with daily

85   mean temperature above 5 °C in a year. The growing season length index, which is based on the growing season start, has been criticized for a high inter-annual variability related to the fact that the index operates on synoptic time scales (Cornes et al., 2019), rather than representing the conditions within a whole season. Thus, we also used the growing degree days index that can be seen as a starting point for spring vegetation based on different thresholds (Wypych et al., 2017).

Table 1. Climate and phenological indices. The phenological model descriptions are found in appendix A

Climate index (Abbr.)	Definition	Units
Growing season start (GSS)	First day of at least 6 days with daily mean temperature > 5 °C	day-of-year
Growing degree days (GDD)	Accumulated temperature > 5 °C reaching 200 GDD	day-of-year
Frost days (FD)	Number of frost days with daily mean temperature $\leq$ 0 °C	days
Last frost day (LFD)	Last day of the first half of the year with daily mean temperature $\leq$ 0 °C	day-of-year
Cold spell index (CSDI)	Number of 5 consecutive days with daily mean temperature > 20th percentile	days
Warm spell index (WSDI)	Number of 5 consecutive days with daily mean temperature < 80th percentile	days
Wet days (WD)	Number of days with daily precipitation $\geq$ 1 mm	days
Snowfall days (SD)	Number of days with daily mean temperature < 2 °C and daily precipitation sum $\geq$ 1 mm	days
Phenological index	**Description and scientific name**	**Model**
Cherry full flowering	Prunus avium - flowering (50 %)	PTT
Beech leaf unfolding	Fagus sylvatica - leaf unfolding (50 %)	TT
Frost index	Accumulated temperature below 0 °C after phenological phase	-

All indices were calculated for the entire available period from 1763 to 2020 and for the months of March to May for
aggregated indices. Long-term changes in the indices were discussed based on 30-year mean values for eight climatological
periods from 1781 to 1810, 1811 to 1840, 1841 to 1870, 1871 to 1900, 1901 to 1930, 1931 to 1960, 1961 to 1990, and 1991
to 2020. Anomalies are shown as a deviation from the pre-industrial reference period of 1871 to 1900 as it is defined in Begert
et al. (2019). For the calculation of indices based on the Swiss Plateau series (Brugnara et al., 2022), the entire year/season was
set to missing for growing season start and growing degree days if a missing value occurred. For aggregated indices (e.g. frost
days, wet days), a value was set to missing if more than 10 % of the values in an aggregation period were missing. Further
definitions can be found in Table 1.

All calculated indices for a monthly, seasonal, and annual time aggregation for the period 1763 to 2020 are published at the
open-access repository PANGAEA (Imfeld et al., 2023a).

3.2 Phenological application

To study the impacts of past weather on the spring vegetation, we calculated the cherry full flowering and beech leaf unfolding
day-of-year from daily mean temperature data. Cherry flowering occurs around mid April in the Swiss plateau and can thus
serve as a good indication for the state of the spring vegetation. Beech leaf unfolding occurs around the beginning of May in
the Swiss plateau and is thus representative of later spring vegetation. The phenological phases refer to the day of the year
when 50 % of the cherry tree is blooming, resp. 50 % of the beech leafs are unfolding. We used the phenological observations
of the Swiss phenological network (SPN) between 1951 and 2020 for calibrating and reconstructing the phenological phases

during the 258-year long period. Only series with a quality class of at least 3 were used leading to a total of 68 (56) time series for cherry flowering (beech leaf unfolding) with record lengths between 35 and 71 years distributed across Switzerland (Auchmann et al., 2018; Brugnara et al., 2020a). For cherry full flowering only grid cells below 1600 m a.s.l. where considered because the observational network only includes observations below this altitude.

110   The cherry full flowering time was estimated using a photo thermal time model (PTT) as implemented in the phenor R package (Hufkens et al., 2018) for which 3 parameters needed to be calibrated (Appendix A, Eq. A1 and Eq. A2). Beech leaf unfolding was estimated using a thermal time model (TT) which also is based on 3 parameters but no term accounting for daylength, i.e. photoperiod (Appendix A, Eq. A1 and Eq. A3). The model parameters were calibrated with a Markov Chain Monte Carlo differential evolution sampler with snooker update (Ter Braak and Vrugt, 2008; Hartig et al., 2023) and run with
115   18000 iteration across 3 chains. Bayesian model calibration has been shown to perform well for the calibration of phenological models (e.g. Meier and Bigler, 2023; Fu et al., 2012) and it further allows for assessing the uncertainty and convergence of model parameters. For the prior distributions of the parameters a uniform distribution with pre-set bounds as defined in Hufkens et al. (2018) were used. The model calibration converged with a potential scale reduction factors of 1.02 or below (Gelman and Rubin, 1992). Figure A1 in Appendix A shows the trace of the calibrated parameters for the 6000 iterations and the marginal
120   densities thereof. Figure A2b shows the root mean square error from a cross-validation based on station data. We added both phenological phases to the provided indices on PANGAEA (Imfeld et al., 2023a), but in the following only discuss cherry full flowering.

For comparing the phenological reconstructions to independent historical observations, we used the time series for full flowering of cherry in Liestal (Canton of Baselland) starting in 1894 (Defila and Clot, 2001) and a composite time series of
125   cherry flowering from different historical sources representative of the Swiss plateau by (Rutishauser et al., 2003; Burgdorf et al., 2023).

The cherry full flowering was further used to study the frost occurrence after flowering that could cause damage to trees. A frost index was calculated following Lhotka and Brönnimann (2020) by accumulating daily mean temperature below 0 °C from the onset of cherry flowering (minus 3 d) until the 30 June. This yielded an estimate of area affected by late frost and
130   intensity of the frost occurring.

4   Results

4.1   Longterm changes in climate and phenological indices

Most climate indices showed few differences in their climatological mean in the first five periods from 1781 to 1900 (Fig. 1). The Swiss climatological reference period from 1871 to 1900 showed slightly colder conditions in some of the indices
135   compared to the earlier periods. Growing degree days were up to five days earlier in the Swiss plateau in the periods between 1781 to 1870 compared to the 1871 to 1900 period, up to four frost days less were registered in these periods, and up to eight warm spell days more. Figure B1 in Appendix B shows the anomalies of the seven periods with respect to the pre-industrial mean period from 1871 to 1900 (Begert et al., 2019).
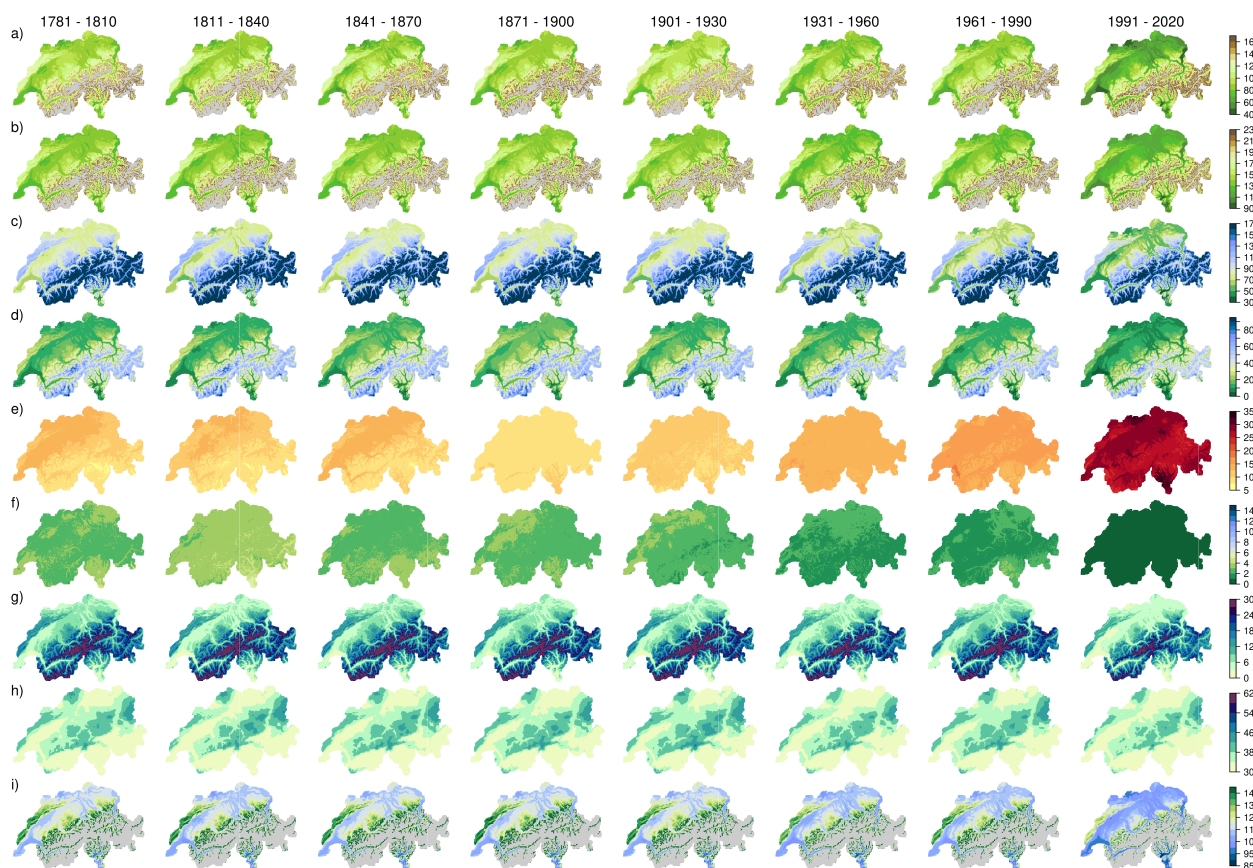
Figure 1. 30-year climatological mean for climate indices for the eight periods between 1781 to 2020. a) Growing season start, b) growing degree days, c) last frost day, d) frost days, e) warm spell duration index, f) cold spell duration index, g) snowfall days, h) wet days, and i) cherry full flowering day-of-year. Light grey areas depict areas, where the indices was not reached in more than 75 % of the years in a period or we did not calculate the index because the grid cells are above 1600 m a.s.l. (last row).

Warmer conditions emerged in all indices for the three periods from 1931 onward. The 1931 to 1960 period showed earlier growing season start and earlier growing degree days compared to the period from 1961 to 1900, but few differences in frost days, last frost days, and warm and cold spells. Very clear differences emerged in the last period of 1991 to 2020 (Fig. 1, last column). Across Switzerland, the growing season started up to 24 d earlier than in the pre-industrial period 1871 to 1900. The 200 GDD was reached up to 25 d earlier, and the last frost days occurred up to 25 d earlier compared to the pre-industrial period 1871 to 1900. Warm spell days increased by up to 20 d, whereas cold spell days decreased by up to 10 d. P values from the comparison of the climatological mean and the pre-industrial mean with a Student's t test show that for most indices the last period significantly differs at a 0.05 confidence level (not shown).

For the precipitation-related indices snowfall days and wet days, differences only ranged between -5 to +5 d throughout all periods (Fig. 1 and B1g and h). The first two periods showed a north-south precipitation difference compared to the

pre-industrial mean, which is likely an artifact of the dataset due to the lack of precipitation data before 1864 in southern
Switzerland. The 1931 to 1960 period showed fewer snowfall days and wet days than the pre-industrial reference period. This
period also included a prolonged episode of warm and dry years between 1945 to 1952 in Switzerland and Western Europe
(Imfeld et al., 2022). The period from 1961 to 1990 showed no differences in snow days compared to the pre-industrial period,
whereas the 1991 to 2020 period showed up to five days fewer snowfall days. Similarly, wet days did not show any difference
in the 1961 to 1990 period, whereas they decreased in the last period. For snowfall days, the differences in the mean value
became significant at a 0.05 level for the last period compared to the pre-industrial reference period (not shown).

Based on our reconstruction, cherry flowering occurred on average between mid and end of April in the Swiss plateau during
the pre-industrial period from 1871 to 1900 (Fig. 1 i). The flowering phase did not show considerable changes in the mean
in the first five periods until 1930. Changes become apparent in the period of 1931 to 1960 at higher locations, and much
more pronounced again in 1991 to 2020 with between 5 and 15 d earlier than in the pre-industrial reference period (see also
Appendix Fig. B1). The Student's t test showed significant differences at a level of 0.05 in parts of Switzerland already in the
1931 to 1960 period (not shown).

Time series for the area-mean of the Swiss plateau region (Swiss recon), for the 20CRv3 reanalysis, the merged time series
from Zurich and Bern (Swiss series), and the ensemble mean of ModE-RA depict a steep trend of the indices in the late 1980s
for daily mean temperature and GDD (Fig. 2a and b). 20CRv3 shows lower temperatures, e.g. leading to later GDD, in the
period from 1806 to around 1835, which is also a period where few observations were assimilated into 20CRv3 (Slivinski et al.,
2021, 2019). ModE-RA agrees well with the Swiss reconstruction and the Swiss series in the 18th and 19th century, whereas
it is on average colder than the other data sets in the 20th century. Notably cold springs in the time series are 1785, which also
showed a much higher number of frost days in the Swiss plateau than any other year, and 1837, which is together with 1785 the
coldest spring in the 258-year-long time series. On the other hand, several springs showed quite high temperatures, comparable
to the beginning of the 21st century. The most prominent among these is the spring of 1862.

The trend towards earlier flowering is also seen in the cherry flowering time series, with much earlier dates after 1989. For the
cherry tree in Liestal, the Pearson correlation between the reconstruction and the observation was 0.85, but the reconstruction
showed a mean bias of 7.36 d (Fig. 2d). For the composite cherry flowering from Rutishauser et al. (2003), Pearson correlation
was 0.67 and the mean bias 2.97 d (Fig. 2e). Despite the biases between the reconstruction and the historical observations, the
phenological reconstruction reproduced the overall variability throughout the years. Thus, the reconstruction offers an estimate
to study cherry flowering in the past across Switzerland. The earliest flowering occurred in 2017 (4 April), which was related to
a damaging frost event in Switzerland (Vitasse and Rebetez, 2018). The latest flowering happened in 1785 (15 May), followed
by 1853 (12 May), and other late years with cherry flowering between 9 and 10 of May were for example 1770 (a prolonged
cold and wet period; see Collet 2018 and Imfeld et al. 2023b), 1817 (after the year without a summer; see Flückiger et al.
2017), 1808, 1932, and 1837.
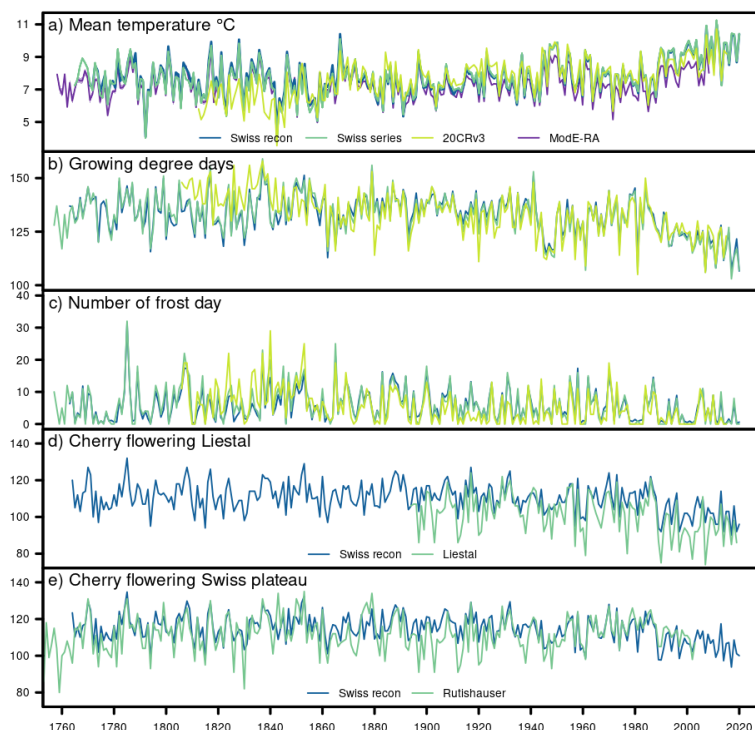
Figure 2. Evolution of indices in the spring season for different data sets. a) Mean temperature, b) growing degree days, c) number of frost days, d) cherry flowering in Liestal for the reconstruction and the observations of Liestal (Defila and Clot, 2001), and f) mean cherry flowering in the Swiss plateau for the reconstruction and the composite series of Rutishauser et al. (2003). Note that for the Swiss series, NA values are removed. The time series of the Swiss gridded reconstruction set cover the area of the Swiss plateau. ModE-RA shows the ensemble mean, and the minimum and maximum member. 20CRv3 shows the ensemble mean and the spread.

4.2 Examples of extreme springs

Based on these climate and phenological indices, we studied three examples of extreme spring conditions, that may affect for example vegetation growth in spring. Namely, we considered the early warm spring in 1862, the occurrence of late frost events in 1873 and 1957, and the three years 1785, 1837, and 1853 with especially cold springs and late cherry flowering. In addition to the presented indices, we analyzed atmospheric variables for illustration of the weather conditions during the extreme spring cases, and we qualitatively evaluated historical sources reporting the weather conditions and weather-related impacts.

4.2.1 The warm spring in 1862

Very warm springs considerably increased after the 1980s (Fig. 2a). However, also in the late 18th and early 19th century several warm springs with high daily mean temperature and for example, early reach of 200 GDD occurred (Fig. 2). The spring of 1862 in particular, stands out with a mean temperature of 10.4 °C between March and May in the Swiss plateau and based

on the gridded reconstruction. It ranks as the third warmest spring since 1763 after the two warmest springs 2011 (11 °C) and 2007 (10.9 °C). With respect to the climatological period 1841 to 1870, 1862 was exceptionally warm with an anomaly of 2.9 °C for the Swiss plateau area mean. In contrast, the second (1841) and third (1846) warmest springs in the 1841 to 1870 period showed less pronounced anomalies of 1.8 and 1.1 °C. The warmest spring in 2011 had an anomaly of only 1.8°C with

195 respect to its mean climate from 1991 to 2020. We also considered the Swiss series of Bern and Zurich (Brugnara et al., 2022) and 2 m temperature from 20CRv3 (Slivinski et al., 2019). In the Swiss series, the spring of 1862 ranks seventh with a mean temperature of 10.09 °C between March and May. It had an anomaly of 2.8 °C considering the mean of the period from 1841 to 1870, whereas 2011 it had an anomaly of 1.8 °C considering its mean climate from 1991 to 2020. Thus, the anomalies were very similar and the spring of 1862 seemed to be unusually warm for this period. In 20CRv3, the anomaly of the spring 1862

200 was lower with 1.9 °C with respect to the 1841 to 1870 period. Across all years, the spring of 1862 only ranks 17th in 20CRv3. In contrast, in ModE-RA, which ends in 2008, the spring of 1862 showed the highest temperature across the period from 1763 to 2008 and had an anomaly of 2.6 °C concerning the 1841 to 1870 mean. The spring of 2007 was the second warmest, but 2011 is missing for comparison. The number of assimilated observations in ModE-RA, however, gradually reduces towards the 21st century affecting the temperature analysis (Valler et al., in review).
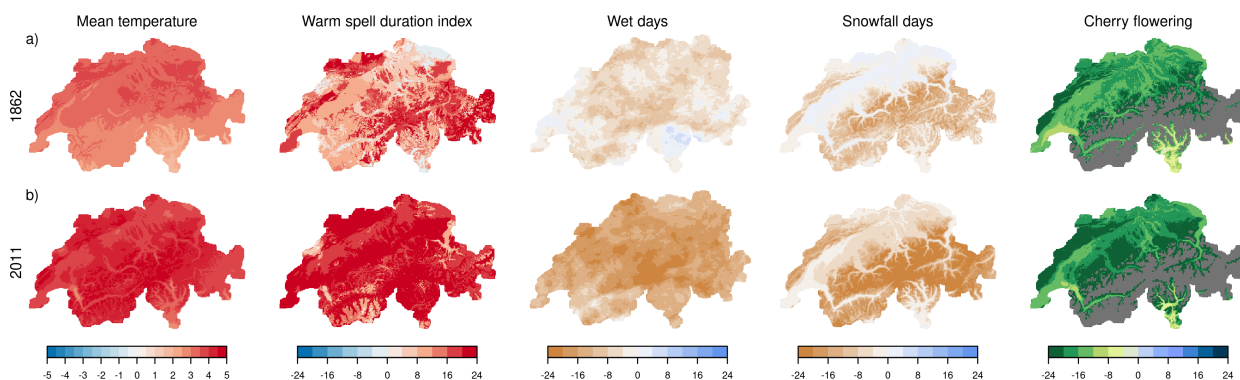
Figure 3. Anomalies of mean seasonal temperature, warm spell duration index, wet days, snowfall days, and cherry flowering date for the two warm springs of a) 1862 and b) 2011. All anomalies are calculated with respect to March to May for the period 1871 to 1900.

205 For both, the warmest spring of 2011 and the warm pre-industrial spring of 1862, climate indices showed above-average temperatures and an above-average number of warm spell days across the entire Switzerland, though much more pronounced in 2011 (Fig. 3). Both springs showed mostly fewer wet days and fewer snowfall days than on average between 1871 and 1900. Cherry flowering was in certain areas up to 24 d advanced, in particular at higher altitudes.

Over eastern Europe, 20CRv3 showed only a very weak positive geopotential height anomaly at the 500hPa level for the

210 mean of the spring months March to May 1862 (Fig. 4a). For the spring of 2011, a more pronounced positive geopotential height anomaly at the 500hPa level was present over western Europe indicating that Switzerland was affected by the warmer and drier conditions (Fig. 4b). In the spring of 1862, a cold anomaly in mid-April interrupted the warm weather (Fig. 4c) leading
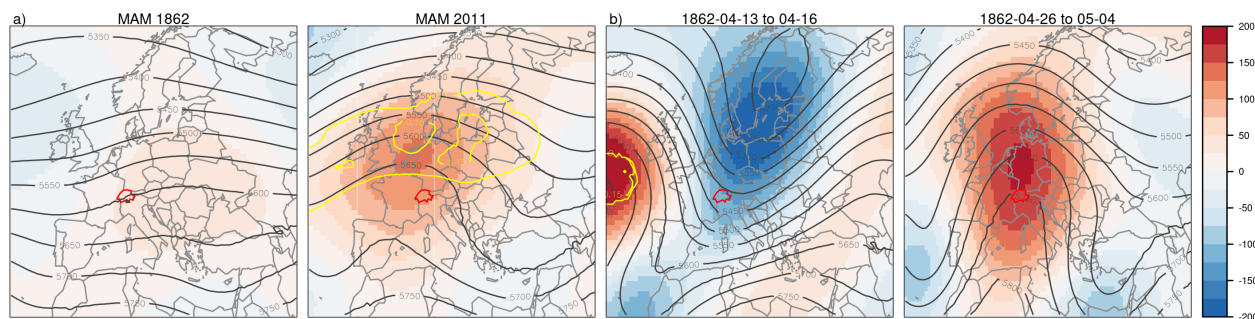
Figure 4. a) Geopotential height field (gpm) at the 500hPa level (contours) and its anomalies (shading) for the March to May mean in 1862 and 2011. b) The period during and after a cold air outbreak in April 1862. Anomalies are calculated with respect to 1871 to 1900. Yellow lines show the blocking frequencies (0.05 and 0.1) across all time steps and all members. The data is from 20CRv3 (Slivinski et al., 2019).

to frost and snowfall over Switzerland, but, for example, for Aarau as mentioned above no reports on vegetation damage were found (Zschokke, 1865). After the cold spell, a pronounced ridge established again over Western Europe leading to the warm

215 spring weather (Fig. 4d). In ModE-RA, for which 1862 is the warmest spring in the 1763 to 2008 period, the geopotential height field of March to May was comparable to 20CRv3. Still, the respective temperature anomalies were more pronounced than in 20CRv3 (see e.g. Fig. 2 and anomalies in the text above) (Appendix, Fig. C1).

Historical sources indeed reported an unusual early snow-free period in spring 1862 in Ursern, a valley in the Canton of Uri (Ambühl, 1961). Already very early in the year the Gotthard was passed by carriage and not sled (Zschokke, 1865) which

220 could point to warm weather leading to early snow-melting, but also to less snowfall in the months before. For Aarau, Theodor Zschokke reported unusual advances in the vegetation, for example, a start of the cherry flowering as early as the 6th of April. In our reconstruction the cherry flowering happened on the 8 April in Aarau and on average on the 11 April in the Swiss plateau. The snowfall and frost that occurred in mid-April did not lead to damage in lower-lying areas (Zschokke, 1865). An official weather report from the weather service for the year 1862, however, did not mention an unusually warm spring (MeteoSwiss,

225 2016), but more qualitative sources describing the spring weather might be available.

4.2.2 The late frost events in 1873 and 1957

Combining the cherry flowering reconstruction with climate indices allows us to look at climate events that affected vegetation directly, such as the occurrence of late frost in spring that can lead to considerable damage to vegetation. Two events stand out when considering the affected area and the intensity of the frost events. In 1873, frost conditions after the cherry flowering

230 affected large parts of Switzerland, however, the temperature did not fall much below 0 °C (daily mean temperature). The frost index based on the accumulated negative temperature reached at most -6 °C in the Swiss Plateau (Fig. 5a). The last frost day occurred between the 26th and 28th of April across northern Switzerland, which is more than half a month later than it occurred on average between 1871 and 1900. In contrast, cherry trees reached their full bloom up to 10 d early. In the spring

of 1957, a frost event occurred with very low temperatures, but the affected area was smaller (Fig. 5b). The frost index showed
235   much higher values, but affecting only areas above 800 m a.s.l. For these areas, the last frost days, which occurred between
the 6th and 8th of May, were also more than half a month later than between 1871 and 1900, and the cherry tree flowering was
considerably earlier.
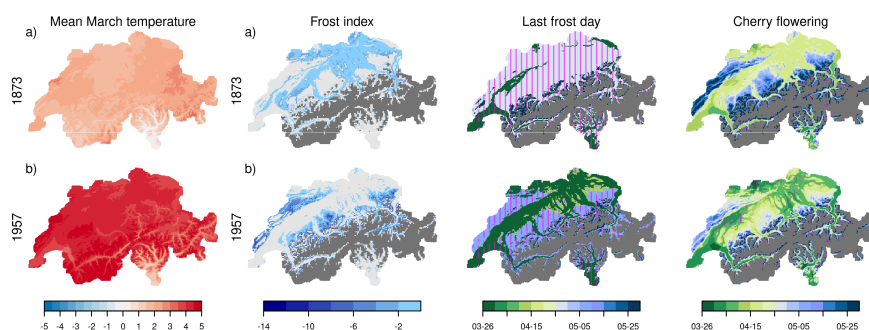
Figure 5. Two frost events causing damage to fruit trees in Switzerland. Temperature anomaly in March with respect to 1871 to 1900, frost index, last frost day, and day of cherry flowering for the two events of a) 1873 and b) 1957. The vertical purple lines indicate areas where frost (cherry flowering) occurred 15 d later (earlier) than the 1871 to 1900 average. The dark grey area denotes grid cells above 1600 m a.s.l.
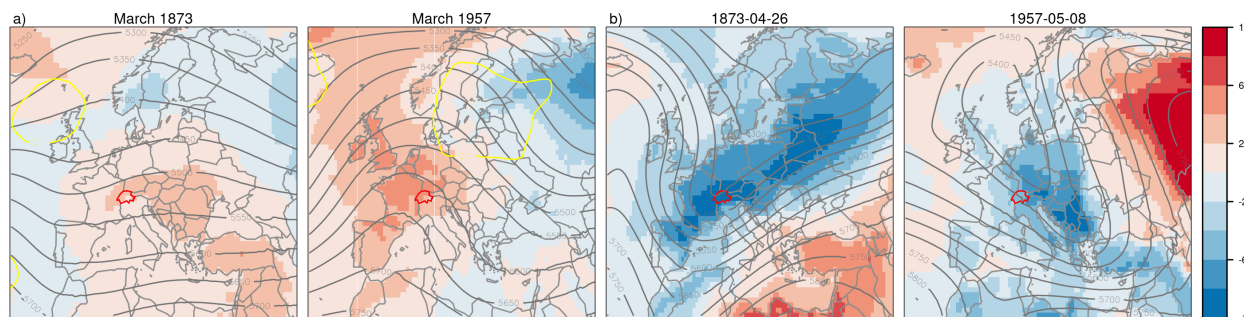
Figure 6. a) 2 m temperature anomalies and geopotential height fields at the 500 hPa level for March of 1873 and 1957. b) Daily 2 m temperature anomalies and daily geopotential height field of the coldest day during the late frost in Bern. Anomalies are calculated with respect to 1871 to 1900. The boundaries of Switzerland are marked in red. The data is from 20CRv3 (Slivinski et al., 2019).

For both springs, March was characterized by average or above-average temperature conditions across Central Europe, though more pronounced for March 1957 (Fig. 5a). These high temperatures in March might have led to an early start of the
240   cherry flowering. In March 1873, temperature anomalies were positive, but the geopotential field shows a more zonal configuration. On the 26th of April 1873, a large trough extended over Switzerland from the Northeast leading to the temperature drop. In 1957, temperatures reached their lowest values on the 8th May when a large trough was located above Switzerland.

For both events, damage caused by the late frost events was reported. In 1873, frost damage was reported for Sursee, Marschlins, Bad-Ragaz, and Appenzell-Innerrhoden, whereas many locations registered snowfall during the 26th to 28th April 245 leading to further damage to the vegetation (Tab. 2). For the frost event of 1957, the Swiss farmer association calculated a reduction of yield in pear and apple trees of 75 % and for cherries of 44 % compared to the six preceding years indicating considerable loss in harvests (Tab. 2).

4.2.3   The cold springs of 1785, 1837, and 1853

The three springs, 1785, 1837, and 1853 registered the lowest temperatures of the entire time series of 258 years and lie below 250 the 1% quantile of all springs temperatures. Their mean temperature in the Swiss plateau from March to May reached only between 4.1 to 5.1 °C (Fig. 2) which is up to 3 °C degrees colder than the 1871 to 1900 average (Fig. 7). In the Swiss series, the coldest spring was in 1837 with a mean temperature of only 3.8 °C and an anomaly of -3.4 °C followed by 1785 with a mean temperature of 4.1 °C and 1853 with a mean temperature of 5.1 °C. In 20CRv3, the spring of 1837 ranks the coldest with an anomaly of -4.0 °C with respect to 1871 to 1900, but 1785 is not available. In ModE-RA, the coldest spring was registered 255 in 1837, followed by 1785, 1970, and 1853 with anomalies between -2.24 and -1.84 °C with respect to 1871 to 1900.
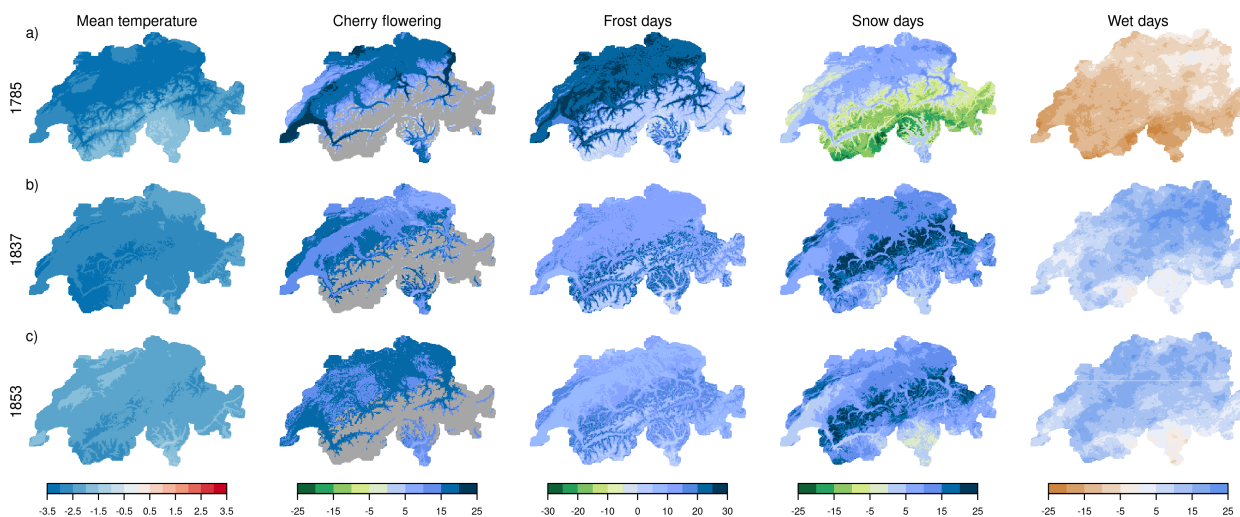
Figure 7. a) Temperature anomaly, b) anomaly in cherry flowering phenology, c) anomaly of the number of frost days, d) anomaly of the number of snow days, e) anomaly of the number of wet days for the cold springs (March to May) of 1785, 1837, 1853. All anomalies are calculated with respect to the 1871 to 1900 climatological mean. Grey areas for cherry flowering denote areas above 1600 m a.s.l.

Indices show, that during the three springs, the cherry flowering was up to 20 d later than the average of 1871 to 1900, and up to 30 more frost days were registered (Fig. 7). Snowfall day anomalies were positive in the spring of 1837 and 1853 mostly in the Alps, but they were negative in the Alps in the spring of 1785. The spring of 1785 also registered fewer wet days than in the 1871 to 1900 period and thus did not concur with the two other springs, that showed wet and cold conditions. In 1785, the frost

260 days indeed showed a different spatial pattern with much larger frost day anomalies in the Swiss plateau region compared to the Alps, which would correspond to an inversion situation. This suggests that synoptic conditions were different over Europe during 1785 compared to the two other cold springs.

Weather types allow a look at the synoptic conditions throughout the three cold springs. The late springs of 1837 and 1853 show a higher occurrence of northerly cyclonic situations (N) and cyclonic situations with westerly flow over Southern

265 Europe (WC) compared to usual spring weather types in the entire period from 1763 to 2020 (see Schwander et al. (2017) for the description of weather types) (Fig. 8a). More cyclonic weather types are found also on average for all springs with temperatures below the 10th quantile (q10). The spring of 1785, however, showed an increase in weather types describing easterly, indifferent flow (E), and high-pressure situations over Europe (HP). To further evaluate this difference in weather types, we used the variance of bandpass-filtered daily pressure observations which give an insight into the "storminess", i.e.

270 the frequency of passing of extra-tropical cyclones. We followed the approach of Brugnara et al. (2015), but only considered station data for calculating anomalies of the standard deviation. The pressure observations show that storminess was decreased for northern stations in 1785, and it was increased for 1837 and 1853 over Switzerland (Fig. 8b). Also, the average of the springs below q10 show increased storminess except for two stations.

This is further confirmed by the monthly fields of geopotential height (anomalies) at the 500hPa level during the three spring

275 months March to May (Fig. 9). In February and March 1785, a trough was present over Central Europe leading to advection of cold air from the north. This situation weakens through April and May, but the trough still remains throughout spring. Stations from several locations in Germany, Poland, and Czech Republic, indeed, show all the same extended negative temperature anomalies throughout March until mid April. In 1837 and 1853, more zonal flow patterns seemed to prevail between March and May and the average of springs below q10 similarly shows more zonal flow.

280 Historical sources confirm these cold spring weather conditions. In spring 1785, for six lakes reports about continued (partial) lake freezing were found until March (see Tab. 2). In March and April, several locations reported abundant snowfall. Due to feed shortage livestock starvation was reported from the Canton of Valais. In St Blaise in the Canton of Neuenburg, strong *Bise* was reported for March and April (Kopp, 1873) and that the first rain (not snow) after 4 months fell at the end of May. Both indicate specific synoptic conditions for this cold spring. For the springs of 1837 and 1853, fewer sources are available, but

285 they reported abundant rain- and snowfall, and frost impacts for various locations in Switzerland. These sources, thus, confirm that all three spring were especially cold and also agree with the classification of Pfister and Wanner (2021) which report cold conditions for all three springs with a category -3 for the Pfister temperature index.

5 Discussion

Climate and phenological indices provide a useful way to study historical extreme spring events, such as cold springs or late
290 frost events and relate them to impacts, for example, the state of vegetation. All indices showed steep changes towards warmer conditions in the last climatological period from 1990 to 2020. These changes in temperature indices correspond to the widely reported trends for temperature development in Switzerland such as in e.g. Isotta et al. (2019) for monthly means, to changes

none
none
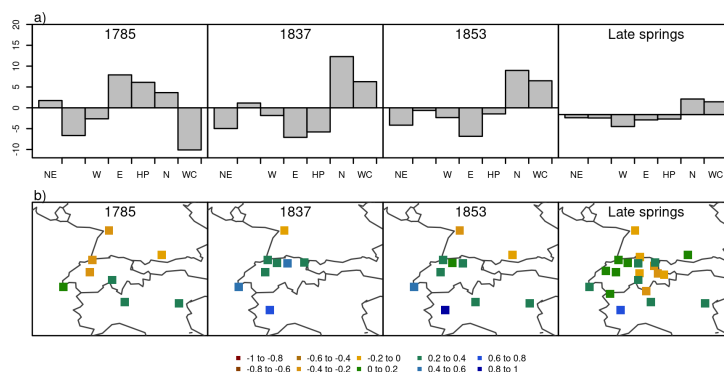
Figure 8. a) Anomalies of weather type frequencies for the three coldest springs and the mean of all springs below q10. The anomalies were calculated with respect to the mean frequency of weather types in March to April from 1763 to 2020 considering all weather types with a cumulative probability of 0.9. NE = Northeast, indifferent; WSW = West-southwest, cyclonic, flat pressure; W = Westerly flow over Northern Europe; E = East, indifferent; HP = High pressure over Europe; N = North, cyclonic; WC = Westerly flow over Southern Europe cyclonic (Schwander et al., 2017). b) Storminess based on pressure observations for the three coldest springs and the mean of the all springs below q10. The anomaly of the standard deviation was calculated with respect to 1961 to 1990 because some series exhibit large gaps between 1871 and 1900.

in snowfall vs. rain (Serquet et al., 2011), and to the changes in spring phenology (Studer et al., 2005; Vitasse et al., 2018). The steep changes towards warmer conditions in the late 1980s have been found in a variety of time series across the world,

295   including vegetation, temperature time series, and snow time series (Reid et al., 2016; Marty, 2008), however, mainly series linked to spring and winter conditions. Sippel et al. (2020) suggested that the changes, which are linked to the cold season temperature, stem from internal variability superimposed on a long-term warming trend.

For Switzerland, phenological models have been used to study for example past frost events (Vitasse et al., 2018) for different tree species and changes in future frost events for grapevines (Meier et al., 2018), but no attempts have been made to extend

300   phenological predictions in space and time. The transferability of the phenological models may be limited in space (e.g. Basler, 2016), and also in time because sensitivities of the calibrated parameters may not be constant over time (Rutishauser et al., 2007). The comparison of historical phenological observations with our reconstruction shows systematic biases of several days for the series of Liestal, but high correlations, thus the reconstruction is able to depict the inter-annual variability of cherry flowering for Liestal. For the composite cherry flowering series, the bias is small with below 3 d, but correlation is also lower.

305   The indices allow us gaining insights into historical springs with unusual weather conditions. The warm spring of 1862 exhibited warm temperatures across the entire Switzerland, which was exceptional for this period, however, it is less exceptional in comparison to the recent warm springs such as 2011 or 2007. Temperature anomalies were high in spring 1862 in the gridded reconstruction, the Swiss series (Brugnara et al., 2022), and ModE-RA, but temperatures anomalies were lower in 20CRv3. The three former data sets are all based on the same temperature series of Bern and Zurich. The geopotential height field in 20CRv3
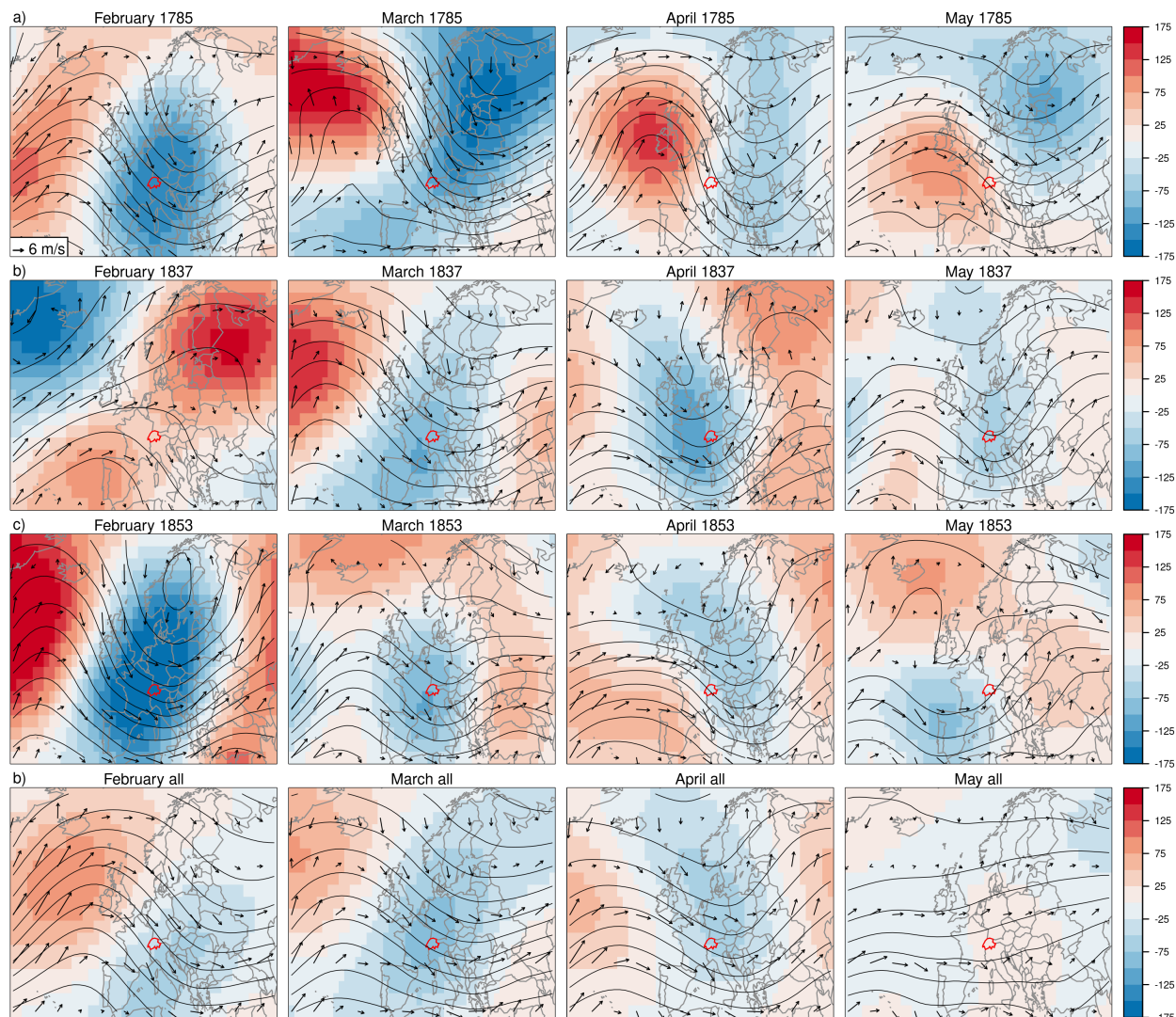
Figure 9. 500 hPa Geopotential height field and wind direction for the months February to May of the three cold springs. Colors show anomalies with respect to the mean of 1871 to 1900, contours show absolute geopotential height field. Arrows show the wind field at 850 hPa. Switzerland is marked in darkred. a) 1785, b) 1837, c) 1853, and d) the composite of all springs below q10. The data is from ModE-RA (Valler et al., in review).

310 does not point towards a exceptionally warm spring of 1862, which shows quite pronounced positive geopotential height anomalies over Europe and a ridge in 2011, but not for the year 1862. Similarly, ModE-RA does not show very pronounced ridge conditions either from March to May, but it does have high temperature anomalies.

Late frost events after a warm period in spring can be particularly damaging for example to fruit harvest. For Switzerland, studies have evaluated how the frost risk has changed over the last decades, and how it may be affected by climate change in the future (Vitasse and Rebetez, 2018; Vitasse et al., 2018; Meier et al., 2018; Lhotka and Brönnimann, 2020), however historical events and their extent have not been studied. These studies rely, though, on daily minimum temperature which has shown different rates of changing compared to daily maximum or daily mean temperature (Scherrer and Begert, 2019). Since minimum temperature is not available in the past, we did not look at changes over time but focus on the representation of specific historical frost events. Two notable frost events occurred in the spring of 1873 and 1957. Harvest data for 1957 showed a considerable loss for apple, pear, and cherry trees (SBV, 1958), which also agrees with the frost index showing strong negative values. For the year 1873, only qualitative descriptions of frost damage was available. Since the frost index is based on daily mean temperature and not minimum temperature, it may not capture the extent of the frost event entirely. But, the data set allowed us to track past frost events based on phenology and frost days and relate them to historical descriptions of the events. This could be done as well for earlier events, such as the late frost in 1802.

Lastly, we considered the three springs 1785, 1837, and 1853 that registered the lowest temperatures from March to May in the Swiss reconstruction. Climate indices showed differences between 1785 and the two springs of 1837 and 1853 with respect to the occurrence of frost days, snowfall days, and wet days. Weather types, the storminess calculation, and the ModE-RA confirmed these differences. The spring of 1785 was under the influence of a pronounced cold trough with a higher occurrence of easterly, high-pressure, and northerly weather types. This led to particular cold, but also dry conditions. The frost day anomalies in the Swiss Plateau indicated likely prolonged inversion, and historical sources describe extended periods of *Bise* which can also lead to inversions and fog in the Swiss plateau. Daily surface pressure fields over Europe would be needed to study the cold conditions in late winter and early spring of 1785 in more detail. In 1837 and 1853, a higher storminess was found in accordance with a more zonal flow and low-pressure systems passing leading to the above-average wet conditions. For the very cold winter of 1785, six of the large lakes of Switzerland reported that the lakes were frozen until March, which would also be indicative of cold winters. As suggested by Franssen and Scherrer (2008) lake freezing could be reproduced based on negative growing degree days for further phenological comparison.

The spring of 1785 followed the cold years after the Laki eruption which occurred in Iceland in 1783 (Yiou et al., 2014; Zambri et al., 2019), but the very cold period end of winter and beginning of spring of 1785 has not been studied in detail. Also, the spring of 1837 followed a volcanic eruption, namely the Cosiguna in Nicaragua in January 1835. After this eruption, several cold years were evident in tree and frost rings from Europe (Longpré et al., 2014). However, Longpré et al. (2014), also stated that a cooling trend was already noted prior to the eruption. The spring of 1853 has not been related to cold conditions in previous literature, and for this spring the three data sets do not agree with respect to the magnitude of the negative temperature anomalies.

These cold spring conditions, in particular the unusually cold conditions in 1785, thus provide a rather unique case of cold spring conditions. Studying such weather in detail could still give relevant insights into mechanisms related to cold spring weather.

6 Conclusions

Climate and phenological indices allow us to depict changes in spring weather and to study extreme springs since the mid-18th century. The 258-year-long time series for the different indices all showed few changes for the first 200 years and a steep increase toward warmer conditions in the most recent decades, which has been shown by many studies. Some extreme spring events were, however, evident from the time series. Based on the different indices, we evaluated three cases of such extreme spring weather conditions since the mid-18th century. The spring of 1862 was exceptionally warm with respect to its climatological mean and it still ranks among today's warmest springs, though this ranking is highly dependent on the dataset. Upper-level atmospheric fields indicate the warm weather conditions in spring 1862, but they are not comparable to the exceptionally warm conditions in spring 2011. The combination of phenology and frost days allows us to evaluate past frost events that caused damage to vegetation. Whereas for the warm summer of 1862, no frost damage was reported despite a cold air outbreak, for the two cases of 1873 and 1957, the frost index shows the affected areas and historical reports confirm the significance of these events.

In the period from 1763 to 2020, three springs showed very cold mean temperature from March to May of at most 5.1 °C. Whereas the springs of 1837 and 1853 showed cold and wet conditions, during spring 1785 fewer wet days than on average from 1871 to 1900 and, thus, dry conditions were registered. An evaluation of weather types, of a storminess index based on bandpass-filtered pressure data, and ModE-RA showed that the 1785 spring was related to more high-pressure conditions and northeasterly flow over Europe, which brought cold air towards Switzerland. The high frost day amounts in the Swiss plateau and reports about *Bise* further suggest a synoptic situation favorable for prolonged inversion and fog in the Swiss plateau in March extending to April. In 1837 and 1853, the zonal flow and mainly cyclonic conditions led to cold but also wet springs. Both, the spring of 1785 and 1837 occurred after volcanic eruptions in the extratropics and the subtropics.

The climate and phenological indices, thus, allowed us to get insights into different historical extreme spring events. It was possible to relate these springs to impacts through historical sources and to evaluate the atmospheric conditions behind them by considering further data sets. Studying such past springs might also nowadays be interesting to better understand the causes of cold and warm springs. Modelling the phenology allowed to relate the historical weather conditions in a straightforward manner to impacts, such as late frost events causing damage to harvests. But, phenological phases can also be relevant for agricultural modelling, and thus, may contribute to agricultural modelling of historical events in more detail.

Appendix A: Phenological models

The cherry full flowering dates are estimated based on the photo thermal time model that has been proposed by various studies
375 to model phenological phases (Basler, 2016; Meier et al., 2018; Hänninen, 1990). It is based on the growing degree days
temperature response and a term that accounts for the photoperiod estimated based on the daylength L_i (Eq. A1 and A2).
Temperatures are accumulated starting at day t_0. When S_{frc} reaches a specific threshold F_{crit}, the phenological phase happens.
The parameters F_{crit}, T_{base}, and t_0 are calibrated based on the phenological observations from 1951 to 2020. The beech leaf
unfolding dates are estimated based on the thermal time model. As for the photo thermal time model, it is based on the growing
380 degree days temperature response, but daylength is not considered (Eq. A1 and A3).

$$R_g(T_i) = \begin{cases} 0 & \text{if } T_i \leq T_{base} \\ T_i - T_{base} & \text{if } T_i > T_{base} \end{cases} \tag{A1}$$

$$S_{frc} = \sum_{n=t_0}^{n} \frac{L_i}{24} R_g \tag{A2}$$

$$S_{frc} = \sum_{n=t_0}^{n} R_g \tag{A3}$$
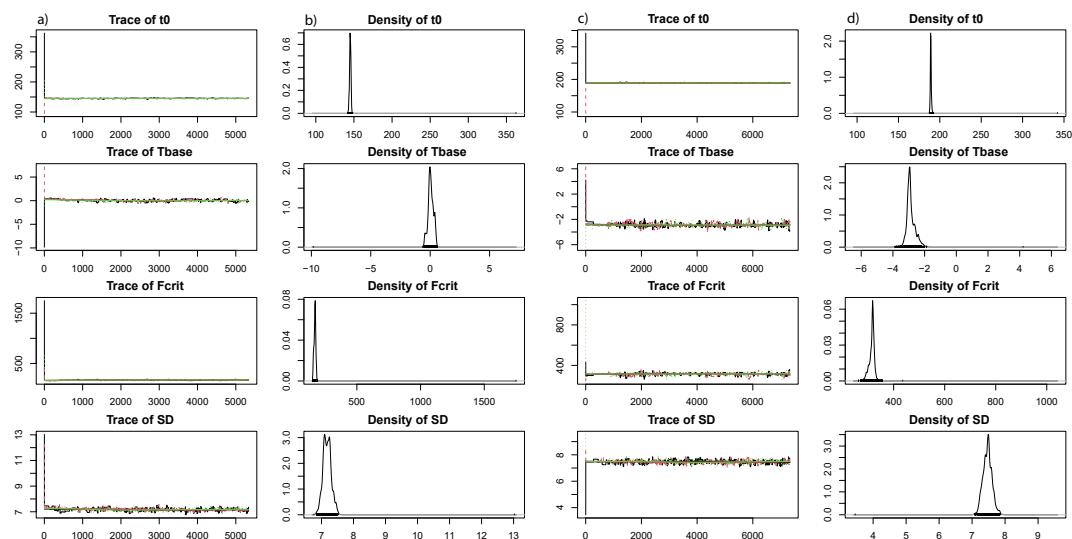
Figure A1. Convergence of the Markov Chain Monte Carlos DEzs algorithm for the calibration of the photo thermal time model (PTT) and the thermal time model (TT). a) Trace of the iterations after burn-in for the three chains and the four parameters. b) Marginal distribution of the four parameters based on the three chains. The first three parameters stem from the model, whereas the standard deviation is estimated during model calibration. See formula in Eq. A2 and A1 for the parameters. Note that t_0 does not start on 1st January, but on 21st September. c and d) are the same as a and b) but for the thermal time model and beech leaf unfolding. Note that we used 8000 iterations of the thermal time model to reach convergence.
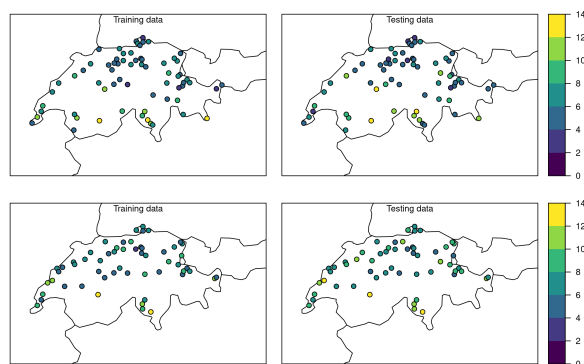
Figure A2. Root mean square error in days of the cross-validation for cherry flowering (upper row) and beech leaf unfolding (lower row) observations from the Swiss Phenology Network for training data (even years/left column) and testing data (odd years/right column).

Table 2. Selection of registered weather impacts for the frost events and cold springs in Switzerland based on the Euro-Climhist database (Pfister et al., 2017) and further sources. The original sources are listed where possible and otherwise secondary sources.

Time	Location	Impacts	Sources
Frost events			
1873 April	Sursee	complete damage of cherry harvest	MZA (1873)
1873 April	Marschlins	damage of walnut trees and grapes	MZA (1873)
1873 April	Switzerland	snow/frost damage on fruit trees and grapes	Appenzeller-Kalender (1874)
1957 April/May	Switzerland	considerable losses in fruit harvest	SBV (1958)
Late springs			
1785 Jan-Apr	Lake Constance	water bodies frozen	Paffrath (1915)
1785 March	Lucerne	water bodies frozen	Staatsarchiv-Lucerne (1755-1829)
1785 March	Geneva	water bodies frozen, ice partially walkable	Forel (1892)
1785 March	Lake Constance	snowfall	Paffrath (1915)
1785 March	Thur river (Ct. of St Gall)	water bodies frozen	Braecker (1998)
1785 March	Lake Alpnach	water bodies frozen	Schaller-Donauer (1937)
1785 March	Lake Zurich	water bodies frozen	Müller (1878)
1785 March	Wattwil (Canton of St Gall)	several reports on abundant snow	Braecker (1998)
1785 March	Chur (Canton of Grisons)	reports on abundant snow, 9 d snowfall	Grimmer (2019)
1785 March	Lake Constance	reports on abundant snowfall	Paffrath (1915)
1785 March	Binn (Canton of Valais)	reports on birds frozen to death	Zennhäuser (2008)
1785 April	Lake Constance	snow impact, abundant snow, livestock starved	Paffrath (1915)
1785 April	Chur (Canton of Grisons)	reports on abundant snow, 6d snowfall	Grimmer (2019)
1785 April	Binn (Canton of Valais)	vegetation delayed, livestock starved	Zennhäuser (2008)
1785 March	St Blaise (Ct. of Neuenburg)	rigorous cold, abundant snow, and strong *Bise*	Kopp (1873)
1785 April	St Blaise (Ct. of Neuenburg)	abundant snow, cold, and strong *Bise*	Kopp (1873)
1785 May	Lake Constance	delayed vegetation and frost impact on vegetation	Paffrath (1915)
1785 May	Wattwil (Canton of St Gall)	fresh snow at higher elevations	Braecker (1998)
1837 March	Canton of Zurich	snow and rain quantities 'as expected for a January'	Vogel (1841)
1837 March	Simplon (Canton of Valais)	13 death due to avalanche	Joller (1888)
1837 April	Canton of Zurich	large snow and rain quantities	Vogel (1841)
1837 May	Canton of Zurich	large snow and rain quantities	Vogel (1841)
1837 May	Grindelwald (Ct. of Bern)	permanent snow cover	Strasser (1890)
1853 May	Canton of Zurich	large snow and rain quantities	Vogel (1841)
1853 May	Grindelwald (Ct. of Bern)	permanent snow cover	Strasser (1890)

Appendix B: Anomaly maps of the calculated climate indices
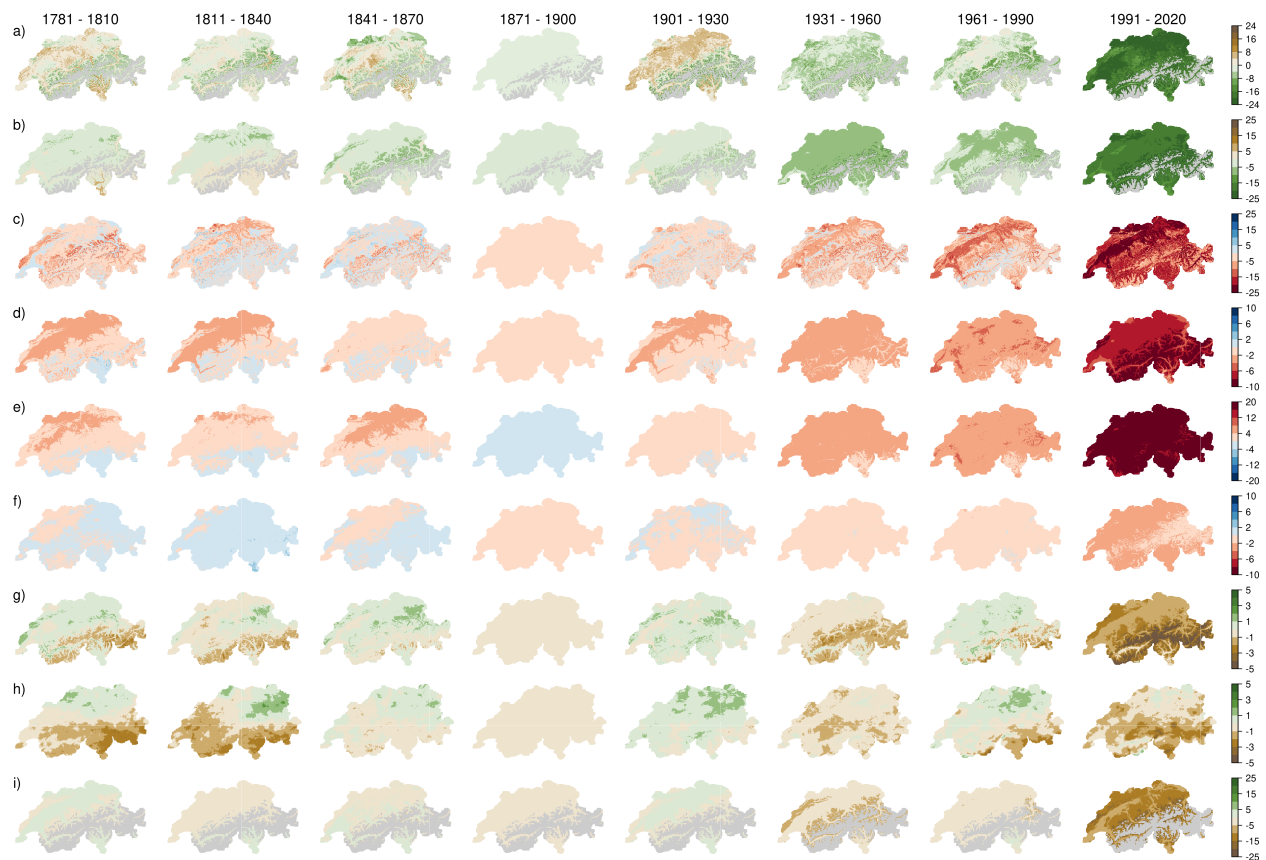
Figure B1. Anomalies of 30-year climatology for climate indices for all six periods with respect to the pre-industrial reference period from 1871 to 1900. a) Growing season start, b) growing degree days, c) last frost day, d) the number of frost days, e) warm spell days, f) cold spell days, g) snowfall days, h) wet days, and i) cherry full flowering. Light grey areas depict areas, where the indices is 0 in more than 75 % of the years in a period or we do not consider it because the grid cells are above 1600 m a.s.l. (last row).

385 Appendix C: The warm spring of 1862 in ModE-RA
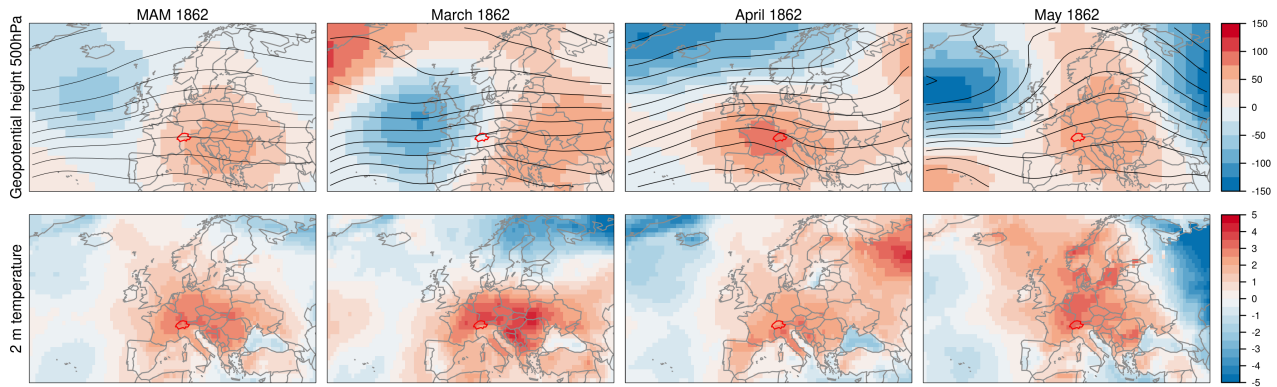
Figure C1. a) Geopotential height anomalies (shading) and absolute values (contour) for the 500hPa level. b) 2 m temperature anomalies. Anomalies are calculated with respect to 1871 to 1900. The borders of Switzerland are marked in darkred. Data is from ModE-RA (Valler et al., in review).

Code availability. The code for the calculation of indices is available on github: https://github.com/imfeldn/swiss_indices

Data availability. Reconstructed daily precipitation and temperature data sets over the period 1763-01-02 to 2020-12-31 are published at the open-access repository PANGAEA under https://doi.org/10.1594/PANGAEA.950236. The climate and phenological indices for the period 1763 to 2020 described in this article are published at the open-access repository PANGAEA under https://doi.org/10.1594/PANGAEA.950236.

Author contributions. NI performed the analyses and wrote the manuscript. KH helped with setting up the calibration of the phenological model and contributed to the manuscript. SB supervised the process and contributed to the manuscript.

Competing interests. The authors declare that they have no conflict of interest.

Acknowledgements. This work was funded by the Swiss National Science Foundation (project "WeaR", grant no. 188701) and by the European Commission through H2020 (ERC Grant PALAEO-RA 787574). The authors acknowledge the data provided by the projects "CHIMES" (SNF grant no. 169676) (Brugnara et al., 2020b), "Long Swiss Meteorological series" funded by MeteoSwiss through GCOS Switzerland (Brugnara et al., 2022), and "DigiHom" (Füllemann et al., 2011).

References

Ambühl, E.: 100 Jahre Einschneien und Ausapern in Andermatt (1860/1960), Die Alpen, https://www.sac-cas.ch/index.php?eID=dumpFile&
    t=f&f=133729&token=e932334ef1e45fb867c0f664f81416f77eea1429, (last accessed 20 June 2023), 1961.

Appenzeller-Kalender: Appenzeller Kalender: Von der Witterung und Fruchtbarkeit vom Herbst 1872-1873, https://doi.org/10.5169/seals-
    373580, 1874.

Auchmann, R., Brugnara, Y., Rutishauser, T., Brönnimann, S., Gehrig, R., Pietragalla, B., Begert, M., Sigg, C., Knechtl, V., Calpini, B., and
    Konzelmann, T.: Quality Analysis and Classification of Data Series from the Swiss Phenology Network, Technical Report Meteoswiss,
    271, 77 pp, https://www.meteoschweiz.admin.ch/dam/jcr:5220f36c-435d-4d46-b766-ba91b0dffe37/fachbericht-271.pdf, (last accessed
    20 June 2023), 2018.

Basler, D.: Evaluating phenological models for the prediction of leaf-out dates in six temperate tree species across central Europe, Agricultural
    and Forest Meteorology, 217, 10–21, https://doi.org/10.1016/j.agrformet.2015.11.007, 2016.

Begert, M., Stöckli, R., and Croci-Maspoli, M.: Klimaentwicklung in der Schweiz - vorindustrielle Referenzperiode und Veränderung
    seit 1864 auf Basis der Temperaturmessung, Technical Report Meteoswiss, 274, 23 pp, https://www.meteoswiss.admin.ch/dam/jcr:
    4c89a839-d577-47f1-aeb9-a30749ddaf2b/AB_Vorind_Refp_v1.1_de.pdf, (last accessed 30 June 2023), 2019.

Braecker, U.: Tagebücher 1779-1788 (Sämtliche Schriften 2), C.H.Beck/Haupt, Muenchen, 1998.

Brown, P. J., Bradley, R. S., and Keimig, F. T.: Changes in Extreme Climate Indices for the Northeastern United States, 1870–2005, Journal
    of Climate, 23, 6555 – 6572, https://doi.org/10.1175/2010JCLI3363.1, 2010.

Brugnara, Y., Auchmann, R., Brönnimann, S., Allan, R. J., Auer, I., Barriendos, M., Bergström, H., Bhend, J., Brázdil, R., Compo, G. P.,
    Cornes, R. C., Dominguez-Castro, F., van Engelen, A. F. V., Filipiak, J., Holopainen, J., Jourdain, S., Kunz, M., Luterbacher, J., Maugeri,
    M., Mercalli, L., Moberg, A., Mock, C. J., Pichard, G., Řezníčková, L., van der Schrier, G., Slonosky, V., Ustrnul, Z., Valente, M. A.,
    Wypych, A., and Yin, X.: A collection of sub-daily pressure and temperature observations for the early instrumental period with a focus
    on the" year without a summer" 1816, Climate of the Past, 11, 1027–1047, https://doi.org/10.5194/cp-11-1027-2015, 2015.

Brugnara, Y., Auchmann, R., Rutishauser, T., Gehrig, R., Pietragalla, B., Begert, M., Sigg, C., Knechtl, V., Konzelmann, T., Calpini, B.,
    and Brönnimann, S.: Homogeneity assessment of phenological records from the Swiss Phenology Network, International journal of
    biometeorology, 64, 71–81, https://doi.org/10.1007/s00484-019-01794-y, 2020a.

Brugnara, Y., Pfister, L., Villiger, L., Rohr, C., Isotta, F. A., and Brönnimann, S.: Early instrumental meteorological observations in Switzer-
    land: 1708–1873, Earth System Science Data, 12, 1179–1190, https://doi.org/10.5194/essd-12-1179-2020, 2020b.

Brugnara, Y., Hari, C., Pfister, L., Valler, V., and Brönnimann, S.: Pre-industrial temperature variability on the Swiss Plateau derived from
    the instrumental daily series of Bern and Zurich, Climate of the Past Discussions, pp. 1–34, https://doi.org/10.5194/cp-2022-34, 2022.

Burgdorf, A.-M., Brönnimann, S., Adamson, G., Amano, T., Aono, Y., Barriopedro, D., Bullón, T., Camenisch, C., Camuffo, D., Daux, V.,
    del Rosario Prieto, M., Dobrovolný, P., Gallego, D., García-Herrera, R., Gergis, Joelle Grab, S., Hannaford, M. J., Holopainen, J., Kelso,
    C., Kern, Z., Kiss, Andrea Kuan-Hui Lin, E., Loader, N. J., Možný, M., Nash, D., Nicholson, S. E., Pfister, C., Rodrigo, F. S., Rutishauser,
    T., Sharma, S., Takács, K., Vargas, E. T., and Vega, I.: DOCU-CLIM: A global documentary climate dataset for climate reconstructions,
    Scientific data, 10, 402, https://doi.org/10.1038/s41597-023-02303-y, 2023.

Collet, D.: Die doppelte Katastrophe: Klima und Kultur in der europäischen Hungerkrise 1770–1772., vol. 18 of *Umwelt und Gesellschaft*,
    Vandenhoeck & Ruprecht, https://doi.org/10.13109/9783666355929, 2018.

Cornes, R. C., van der Schrier, G., and Squintu, A. A.: A reappraisal of the thermal growing season length across Europe, International
435   Journal of Climatology, 39, 1787–1795, https://doi.org/10.1002/joc.5913, 2019.

Defila, C. and Clot, B.: Phytophenological trends in Switzerland, International journal of biometeorology, 45, 203–207,
https://doi.org/10.1007/s004840100101, 2001.

Diodato, N., Fratianni, S., and Bellocchi, G.: Reconstruction of snow days based on monthly climate indicators in the Swiss pre-alpine
region, Regional Environmental Change, 20, 1–9, https://doi.org/10.1007/s10113-020-01639-0, 2020.

440   Domínguez-Castro, F., Reig, F., Vicente-Serrano, S. M., Aguilar, E., Peña-Angulo, D., Noguera, I., Revuelto, J., van der Schrier, G., and
El Kenawy, A. M.: A multidecadal assessment of climate indices over Europe, Scientific data, 7, 125, https://doi.org/10.1038/s41597-020-
0464-0, 2020.

Flückiger, S., Brönnimann, S., Holzkämper, A., Fuhrer, J., Krämer, D., Pfister, C., and Rohr, C.: Simulating crop yield losses in Switzer-
land for historical and present Tambora climate scenarios, Environmental Research Letters, 12, 074 026, https://doi.org/10.1088/1748-
445   9326/aa7246, 2017.

Forel, F.-A.: Le Léman : monographie limnologique, F. Rouge, Lausanne, https://doi.org/10.5962/bhl.title.124608, 1892.

Franssen, H. J. H. and Scherrer, S. C.: Freezing of lakes on the Swiss plateau in the period 1901–2006, International Journal of Climatology,
28, 421–433, https://doi.org/https://doi.org/10.1002/joc.1553, 2008.

Fu, Y. H., Campioli, M., Demarée, G., Deckmyn, A., Hamdi, R., Janssens, I. A., and Deckmyn, G.: Bayesian calibration of the Unified
450   budburst model in six temperate tree species, International journal of biometeorology, 56, 153–164, https://doi.org/10.1007/s00484-011-
0408-7, 2012.

Füllemann, C., Begert, M., Croci-Maspoli, M., and Bönnimann, S.: Digitalisieren und Homogenisieren von historischen Klima-
daten des Swiss NBCN: Resultate aus DigiHom, Arbeitsberichte der MeteoSchweiz, 236, https://www.meteoswiss.admin.ch/dam/jcr:
c0d90a48-a05d-4ac9-9cf3-10769270d75e/ab236.pdf, (last accessed 21 June 2023), 2011.

455   Gelman, A. and Rubin, D. B.: Inference from iterative simulation using multiple sequences, Statistical science, 7, 457–472,
https://doi.org/10.1214/ss/1177011136, 1992.

Grimmer, M.: The Meteorological Diaries of Johann Rudolf von Salis-Marschlins 1781-1800, Master's Thesis, University of Bern, https:
//occrdata.unibe.ch/students/theses/msc/283.pdf, 2019.

Hänninen, H.: Modelling bud dormancy release in trees from cool and temperate regions, Acta Forestalia Fennica, pp. 1–47,
460   https://doi.org/10.14214/aff.7660, 1990.

Hartig, F., Minunno, F., Paul, S., Cameron, D., Ott, T., and Pichler, M.: BayesianTools: General-purpose MCMC and SMC samplers and
tools for Bayesian statistics, R package version 0.1.8, https://github.com/florianhartig/bayesiantools, 2023.

Hufkens, K., Basler, D., Milliman, T., Melaas, E. K., and Richardson, A. D.: An integrated phenology modelling framework in r, Methods in
Ecology and Evolution, 9, 1276–1285, https://doi.org/10.1111/2041-210X.12970, 2018.

465   Imfeld, N., Hufkens, K., and Brönnimann, S.: Daily gridded temperature, precipitation, and phenology indices for Switzerland from 1763 to
2020, PANGAEA [data set], (in review).

Imfeld, N., Stucki, P., Brönnimann, S., Bader, S., Bürgi, M., Calanca, P., Gubler, S., Holzkämper, A., Hövel, L., Isotta, F. A., Kestenholz, C.,
Kotlarski, S., Mastai, A., Nussbaumer, S. U., Raible, C. C., Röthlisberger, M., Scherrer, S. C., Staub, K., Vicedo-Cabrera, A. M., Vogel,
M.-M., Wehrli, K., Thomas, W., and Zumbühl, H. J.: Hot and dry summers in Switzerland. Causes and impacts of the record summers
470   1947, 2003, and 2018, Bern: Geographica Bernensia, Reihe G Grundlagenforschung G96, https://doi.org/10.4480/GB2022.G98.02, 2022.

Imfeld, N., Pfister, L., Brugnara, Y., and Brönnimann, S.: A 258-year-long data set of temperature and precipitation fields for Switzerland since 1763, Climate of the Past, 19, 703–729, https://doi.org/10.5194/cp-19-703-2023, 2023.

Isotta, F. A., Begert, M., and Frei, C.: Long-term consistent monthly temperature and precipitation grid data sets for Switzerland over the past 150 years, Journal of Geophysical Research: Atmospheres, 124, 3783–3799, https://doi.org/10.1029/2018JD029910, 2019.

475 Joller, F. J.: Collectaneen von Pfarrer Joller, Archiv des Geschichtsforschenden Vereins von Oberwallis, 5, 1888.

Kopp, C.: Résumé des observations météorologiques faites à Neuchâtel dans le 18ème siècle de 1760 à 1800, Bulletin de la Société Neuchâteloise de Sciences Naturelles, 9, 56–67, https://doi.org/10.5169/seals-88065, 1873.

Lhotka, O. and Brönnimann, S.: Possible Increase of Vegetation Exposure to Spring Frost under Climate Change in Switzerland, Atmosphere, 11, https://doi.org/10.3390/atmos11040391, 2020.

480 Longpré, M.-A., Stix, J., Burkert, C., Hansteen, T., and Kutterolf, S.: Sulfur budget and global climate impact of the A.D. 1835 eruption of Cosigüina volcano, Nicaragua, Geophysical Research Letters, 41, 6667–6675, https://doi.org/10.1002/2014GL061205, 2014.

Marty, C.: Regime shift of snow days in Switzerland, Geophysical Research Letters, 35, https://doi.org/10.1029/2008GL033998, 2008.

Meier, M. and Bigler, C.: Process-oriented models of autumn leaf phenology: ways to sound calibration and implications of uncertain projections, EGUsphere, 2023, 1–43, https://doi.org/10.5194/egusphere-2022-1423, 2023.

485 Meier, M., Fuhrer, J., and Holzkämper, A.: Changing risk of spring frost damage in grapevines due to climate change? A case study in the Swiss Rhone Valley, International journal of biometeorology, 62, 991–1002, https://doi.org/10.1007/s00484-018-1501-y, 2018.

MeteoSwiss: Witterungsberichte Schweiz 1861 – 1869, https://www.meteoswiss.admin.ch/dam/jcr: a4f1eb74-3a40-4476-bc56-64a27382bb5f/Witterungsberichte_1861-1869.pdf, (last accessed 25 July 2023), 2016.

MeteoSwiss: Documentation of MeteoSwiss Grid-Data Products. Daily Precipitation (final analysis): RhiresD, https://www.meteoswiss. 490 admin.ch/dam/jcr:4f51f0f1-0fe3-48b5-9de0-15666327e63c/ProdDoc_RhiresD.pdf, (last accessed 30 June 2022), 2021a.

MeteoSwiss: Documentation of MeteoSwiss Grid-Data Products. Daily Mean, Minimum and Maximum Temperature: TabsD, TminD, TmaxD, ://www.meteoswiss.admin.ch/dam/jcr:818a4d17-cb0c-4e8b-92c6-1a1bdf5348b7/ProdDoc_TabsD.pdf, (last accessed 30 June 2022), 2021b.

MZA: Schweizerische Meteorlogische Beobachtungen, Annalen der Schweizerisch Meteorlogischen Zentralanstalt, https://www. 495 meteoschweiz.admin.ch/assets/weather-archive/annalen-1873.pdf, (last accessed 25 July 2025), 1873.

Müller, C.: Joh. Heinrich Waser, der zürcherische Volkswirthschafter des 18. Jahrhunderts, seine Bestrebungen und Schicksale und sein statistischer Nachlass, fortgeführt bis zur Gegenwart, J.Herzog, Zurich, 1878.

Paffrath, J.: Schriften des Vereins für die Geschichte des Bodensees und seiner Umgebung, chap. Zum Wetterverlauf am Bodensee, Kommissionsverlag von Joh. Thom. Stettner, Lindau, 1915.

500 Parker, D. E., Legg, T. P., and Folland, C. K.: A new daily central England temperature series, 1772–1991, International Journal of Climatology, 12, 317–342, https://doi.org/10.1002/joc.3370120402, 1992.

Pfister, C. and Wanner, H.: Climate and Society in Europe: The Last Thousand Years, Haupt Verlag Bern, 2021.

Pfister, C., Rohr, C., and Jover, A. C. C.: Euro-Climhist: eine Datenplattform der Universität Bern zur Witterungs-, Klima-und Katastrophengeschichte, Wasser Energie Luft, 109, https://doi.org/10.7892/boris.97013, 2017.

505 Reid, P. C., Hari, R. E., Beaugrand, G., Livingstone, D. M., Marty, C., Straile, D., Barichivich, J., Goberville, E., Adrian, R., Aono, Y., Brown, R., Foster, J., Groisman, P., Hélaouët, P., Hsu, H.-H., Kirby, R., Knight, J., Kraberg, A., Li, J., Lo, T.-T., Myneni, R. B., North, R. P., Pounds, J. A., Sparks, T., Stübi, R., Tian, Y., Wiltshire, K. H., Xiao, D., and Zhu, Z.: Global impacts of the 1980s regime shift, Global Change Biology, 22, 682–703, https://doi.org/10.1111/gcb.13106, 2016.

Rutishauser, T., Luterbacher, J., and Wanner, H.: A 280-Year Long Series of Phenological Observations of Cherry Tree Blossoming Dates for Switzerland, in: Diploma thesis, University of Bern, pp. 1–122, 2003.

Rutishauser, T., Luterbacher, J., Jeanneret, F., Pfister, C., and Wanner, H.: A phenology-based reconstruction of interannual changes in past spring seasons, Journal of Geophysical Research: Biogeosciences, 112, https://doi.org/10.1029/2006JG000382, 2007.

SBV: Statistische Erhebungen und Schätzungen auf dem Gebiete der Landwirtschaft, 35. Jahresheft, p. 41 pp, https://www.sbv-usp.ch/fileadmin/sbvuspch/04_Medien/Publikationen/SES/Archiv/SES_1958-35.pdf, (last accessed, 10 April 2023), 1958.

Schaller-Donauer, A.: Chronik der Naturereignisse im Urnerland 1000-1800, Gotthardpost, 1937.

Scherrer, S. C. and Begert, M.: Effects of large-scale atmospheric flow and sunshine duration on the evolution of minimum and maximum temperature in Switzerland, Theoretical and Applied Climatology, 138, 227–235, https://doi.org/10.1007/s00704-019-02823-x, 2019.

Schwander, M., Brönnimann, S., Delaygue, G., Rohrer, M., Auchmann, R., and Brugnara, Y.: Reconstruction of Central European daily weather types back to 1763, International Journal of Climatology, 37, 30–44, https://doi.org/10.1002/joc.4974, 2017.

Serquet, G., Marty, C., Dulex, J.-P., and Rebetez, M.: Seasonal trends and temperature dependence of the snowfall/precipitation-day ratio in Switzerland, Geophysical Research Letters, 38, L07 703, https://doi.org/10.1029/2011GL046976, 2011.

Sippel, S., Fischer, E. M., Scherrer, S. C., Meinshausen, N., and Knutti, R.: Late 1980s abrupt cold season temperature change in Europe consistent with circulation variability and long-term warming, Environmental Research Letters, 15, 094 056, https://doi.org/10.1088/1748-9326/ab86f2, 2020.

Slivinski, L. C., Compo, G. P., Whitaker, J. S., Sardeshmukh, P. D., Giese, B. S., McColl, C., Allan, R., Yin, X., Vose, R., Titchner, H., Kennedy, J., Spencer, L. J., Ashcroft, L., Brönnimann, S., Brunet, M., Camuffo, D., Cornes, R., Cram, T. A., Crouthamel, R., Domínguez-Castro, F., Freeman, J. E., Gergis, J., Hawkins, E., Jones, P. D., Jourdain, S., Kaplan, A., Kubota, H., Le Blancq, F., Lee, T.-C., Lorrey, A., Luterbacher, J., Maugeri, M., Mock, C. J., Kent Moore, G., Przybylak, R., Pudmenzky, C., Reason, C., Slonosky, V. C., Smith, C. A., Tinz, B., Trewin, B., Valente, M. A., Wang, X. L., Wilkinson, C., Wood, K., and Wyszyński, P.: Towards a more reliable historical reanalysis: Improvements for version 3 of the Twentieth Century Reanalysis system, Quarterly Journal of the Royal Meteorological Society, 145, 2876–2908, https://doi.org/10.1002/qj.3598, 2019.

Slivinski, L. C., Compo, G. P., Sardeshmukh, P. D., Whitaker, J., McColl, C., Allan, R., Brohan, P., Yin, X., Smith, C., Spencer, L., , Vose, R. S., Rohrer, M., Conroy, R. P., Schuster, D. C., Kennedy, J. J., Ashcroft, L., Brönnimann, S., Brunet, M., Camuffo, D., Cornes, R., Cram, T. A., Domínguez-Castro, F., Freeman, J. E., Gergis, J., Hawkins, E., Jones, P. D., Kubota, H., Lee, T. C., Lorrey, A. M., Luterbacher, J., Mock, C. J., Przybylak, R. K., Pudmenzky, C., Slonosky, V. C., Tinz, B., Trewin, B., Wang, X. L., Wilkinson, C., Wood, K., and Wyszyński, P.: An evaluation of the performance of the twentieth century reanalysis version 3, Journal of Climate, 34, 1417–1438, https://doi.org/10.1175/JCLI-D-20-0505.1, 2021.

Staatsarchiv-Lucerne: Unterschiedliche Begebenheiten und Ereignisse des Wetters, teils in Regen- teils in Schneewetter, wie auch in Kälte und Erdstössen (1755-1829), 1755-1829.

Strasser, G.: Grindelwaldner Chroniken, Gletschermann. Familienblatt für Grindelwald, https://doi.org/10.3931/e-rara-78062, 1890.

Studer, S., Appenzeller, C., and Defila, C.: Inter-annual variability and decadal trends in alpine spring phenology: a multivariate analysis approach, Climatic Change, 73, 395–414, https://doi.org/10.1007/s10584-005-6886-z, 2005.

Ter Braak, C. J. and Vrugt, J. A.: Differential evolution Markov chain with snooker updater and fewer chains, Statistics and Computing, 18, 435–446, https://doi.org/10.1007/s11222-008-9104-9, 2008.

Valler, V., Franke, J., Brugnara, Y., Samakinwa, E., Hand, R., Lundstad, E., Burgdorf, A.-M., and Brönnimann, S.: ModE-RA – A global monthly paleo-reanalysis of the modern era (1421 to 2008), Sci. Data, in review.

Vitasse, Y. and Rebetez, M.: Unprecedented risk of spring frost damage in Switzerland and Germany in 2017, Climatic Change, 149, 233–246, https://doi.org/10.1007/s10584-018-2234-y, 2018.

Vitasse, Y., Schneider, L., Rixen, C., Christen, D., and Rebetez, M.: Increase in the risk of exposure of forest and fruit trees to spring frosts at higher elevations in Switzerland over the last four decades, Agricultural and Forest Meteorology, 248, 60–69, https://doi.org/10.1016/j.agrformet.2017.09.005, 2018.

Vogel, F.: Memorabilia Tigurina oder Chronik der Denkwürdigkeiten der Stadt und Landschaft Zürich, im Verlag des Verfassers und in Commission bey S. Höhr, https://doi.org/10.3931/e-rara-26390, 1841.

Wypych, A., Sulikowska, A., Ustrnul, Z., and Czekierda, D.: Variability of growing degree days in Poland in response to ongoing climate changes in Europe, International Journal of Biometeorology, 61, 49–59, https://doi.org/10.1007/s00484-016-1190-3, 2017.

Yiou, P., Boichu, M., Vautard, R., Vrac, M., Jourdain, S., Garnier, E., Fluteau, F., and Menut, L.: Ensemble meteorological reconstruction using circulation analogues of 1781–1785, Climate of the Past, 10, 797–809, https://doi.org/10.5194/cp-10-797-2014, 2014.

Zambri, B., Robock, A., Mills, M. J., and Schmidt, A.: Modeling the 1783–1784 Laki Eruption in Iceland: 2. Climate Impacts, Journal of Geophysical Research: Atmospheres, 124, 6770–6790, https://doi.org/10.1029/2018JD029554, 2019.

Zennhäuser, G.: Witterung und Klima eines Walliser Alpentals nach Aufzeichnungen (1770-1812) des Weibels Johann Ignaz Inderschmitten von Binn, Blätter aus der Walliser Geschichte 40, 40, https://doc.rero.ch/record/200964, (last accessed 12 September 2023), 2008.

Zhang, X., Alexander, L., Hegerl, G. C., Jones, P., Tank, A. K., Peterson, T. C., Trewin, B., and Zwiers, F. W.: Indices for monitoring changes in extremes based on daily temperature and precipitation data, WIREs Climate Change, 2, 851–870, https://doi.org/10.1002/wcc.147, 2011.

Zschokke, T.: Witterungsbeobachtungen in Aarau in den Jahren 1861-1865, vol. 1, Aarau, Sauerländer, https://abn-primo.hosted.exlibrisgroup.com/permalink/f/17uelnu/41ABN_ALEPH_DS000261569, 1865.

Zubler, E. M., Scherrer, S. C., Croci-Maspoli, M., Liniger, M. A., and Appenzeller, C.: Key climate indices in Switzerland; expected changes in a future climate, Climatic change, 123, 255–271, https://doi.org/10.1007/s10584-013-1041-8, 2014.